Forecasting the duration of volcanic eruptions: an empirical probabilistic model

Forecasting the duration of volcanic eruptions: An empirical probabilistic model

L.S. Gunn[1*], S. Blake[1], M.C. Jones[2], H. Rymer[1]

[1] Department of Environment, Earth and Ecosystems, The Open University, Walton Hall, Milton Keynes MK7 6AA, UK [2] Department of Mathematics and Statistics, The Open University, Walton Hall, Milton Keynes MK7 6AA, UK

[*]Corresponding author

email: Leanne.Gunn@open.ac.uk

phone: +44 1908 653429

fax: +44 1908 655151

List of Figures

1 Sketch map of Mt. Etna based on Romano et al. (1979) and Branca et al. (2011) showing the extent of erupted material and the position of their vents/fissures (stars/ yellow lines) for the eruptions within Table 2. Dashed lines represent the boundaries between sectors A, B and C (discussed in the text), VDB = Valle del Bove, VDL = Valle del Leone and VDC = Valle del Calanna 28

2 (a) Plot of cumulative eruption number against eruption start year of all 77 flank eruptions reported between 1300 and 2010. Pale symbols represent the 15 eruptions excluded from this study due to insufficient information regarding their start and/or end date. (b) Plot of eruption duration (on a log scale) against start year for the 62 eruptions included in this study (Table 2). Vertical dashed lines in both plots represent the years 1600, 1670 and 1971 29

3 Empirical survivor function curves for preferred eruption durations from 1600-2010 along with curves for their maximum and minimum possible eruption durations when uncertainty is taken into account (data from Table 2) 30

4 Empirical survivor function curves for eruption durations from 1600-1670 ($n = 7$), 1670-1971 ($n = 31$) and from 1971-2010 ($n = 21$) (data from Table 2) 30

5 Empirical survivor function curves for eruption durations within sectors A ($n = 23$), B ($n = 29$) and C ($n = 6$) between the years 1600 and 2010 (data from Table 2) 31

6 Empirical survivor function (Emp_SF) curves along with their best-fit log-logistic survivor function curves for historical flank eruption durations at Mt Etna (data from Table 2) from (a) 1600-2010 (β = 0.94, σ = 40.56) and (b) 1670-2010 (β = 1.00, σ = 33.00) 32

List of Tables

1 Table of assigned dates and uncertainties 33

2 Dataset of historical Etna flank eruptions with known durations, 1300-2010 34

3 Mantel-Haenszel Logrank test results for all possible sector pairs 42

4 Table showing the forecast results for the 1600-2010 and 1670-2010 datasets using (a) survivor function models, (b) residual life function models where t = 14 days and (c) quantile function models. The first column refers to the scenario being forecast where x is the total eruption duration and p the quantile of interest. CI represents the confidence interval 43

5 Table containing the equations involved in calculating variance ($\hat{V}$) for the Log-logistic distribution in the survivor function ($\hat{F}(x)$), residual life function ($\hat{F}_t$) and quantile function (x_p) models 44

Abstract

The ability to forecast future volcanic eruption durations would greatly benefit emergency response planning prior to and during a volcanic crises. This paper introduces a probabilistic model to forecast the duration of future and on-going eruptions. The model fits theoretical distributions to observed duration data and relies on past eruptions being a good indicator of future activity. A dataset of historical Mt. Etna flank eruptions is presented and used to demonstrate the model. The data has been compiled through critical examination of existing literature along with careful consideration of uncertainties on reported eruption start and end dates between the years 1300 AD and 2010 and data following 1600 is considered to be reliable and free of reporting biases. The distribution of eruption durations between the years 1600 and 1670 is found to be statistically different from that following 1670 and represents the culminating phase of a century-scale cycle. The forecasting model is run on two datasets of Mt. Etna flank eruption durations; 1600-2010 and 1670-2010. Each dataset is modelled using a log-logistic distribution with parameter values found by maximum likelihood estimation. Survivor function statistics are applied to the model distributions to forecast (a) the probability of an eruption exceeding a given duration, (b) the probability of an eruption that has already lasted a particular number of days exceeding a given total duration and (c) the duration with a given probability of being exceeded. Results show that excluding the 1600-1670 data has little effect of the forecasting model result, especially where short durations are involved. By assigning the terms 'likely' and 'unlikely' to probabilities of 66 % and 33 %, respectively the forecasting model is used on the 1600-2010 dataset to indicate that a future flank eruption on Mt. Etna would be likely to exceed 20 days (+/- 7 days) but unlikely to exceed 68 days (+/- 29 days). This model can easily be adapted for use on other highly active, well-documented volcanoes or for different duration data such as the duration of explosive episodes or the duration of repose periods between eruptions.

Key Words Etna, Eruption duration, Probabilistic forecasts, Volcanic hazards

Introduction

The anticipated duration of future or on-going volcanic eruptions is often a topic of much concern in volcanically active areas, yet systematic studies of eruption duration are rare (Mulargia et al. 1985; Stieltjes and Moutou 1989; Simkin 1993; Sparks and Aspinall 2004). Analyses of eruption durations can provide probabilistic constraints on the likely duration of future or on-going eruptions which could greatly benefit emergency response planning at times of volcanic crisis. Although much research has been done on forecasting the likely start of eruptions using statistical analysis of repose intervals (see Marzocchi and Bebbington (2012) for a review), the same cannot be said for duration data as a tool for forecasting the ends of eruptions. The aims of this paper are therefore to present a set of duration data and use it to illustrate a general statistical method of forecasting likely duration (independent of any other information) using Mt. Etna as a case study, chosen for its well documented historical record.

The duration of a volcanic eruption can be defined as the period of time when fresh volcanic material is being emitted at the Earth's surface. Here we consider a period of continuous magma discharge as the basic building block of an eruption. However, the intensity of volcanic activity during an eruption is rarely constant. More often, discrete phases of heightened activity separated by periods of surface quiescence lasting hours, days or months can be observed (Simkin 1993; Siebert et al. 2010). The Smithsonian Institution's Global Volcanism Program considers eruptive phases separated by periods of quiescence of less than 3 months as the same eruption, unless there are significant reasons to treat them as distinct events (Venzke et al. 2002; Siebert et al. 2010). However, the degree and duration of a quiescent pause required to warrant grouping a series of eruptive phases as one eruption, or splitting a series of eruptive phases into more than one eruption, is likely to depend on local circumstances. A similar argument applies to defining durations of repose periods.

This paper begins by critically assessing the available data on the duration of flank eruptions at Mt.

Etna and presents a list of reliable eruption duration data. It goes on to describe and summarise these data using empirical survivor function plots and to assess variations in the distribution of eruption duration with time and location. The paper ends by demonstrating how survivor function statistics can be used to forecast the duration of future and on-going eruptions. Although the focus of this paper is Mt. Etna, the methods used to describe and forecast eruption durations are applicable to other volcanoes with well documented historical activity.

Data selection

Mt. Etna background

Mt. Etna is the most active volcano in Europe, and consequently it is one of the most widely studied and documented volcanoes in the world (Andronico and Lodato, 2005). Hazard studies of Mt Etna began in the late 1970's and early 1980's focussing on patterns in historic eruptions and predicting the location of future activity (Frazzetta and Romano 1978; Guest and Murray 1979; Duncan et al. 1981). Since then numerous studies have built on this work by analysing catalogues of historic eruptions (Mulargia et al. 1985; Behncke and Neri 2003; Branca and Del Carlo 2004; Branca and Del Carlo 2005; Salvi et al. 2006; Neri et al. 2011; Smethurst et al. 2009; Passarelli et al. 2010; Proietti et al. 2011) and producing susceptibility and probabilistic hazard maps of surrounding areas (Andronico and Lodato 2005; Bisson et al. 2009; Behncke et al. 2005; Crisci et al. 2010; Harris et al. 2011; Cappello et al. 2012; Cappello et al. 2013).

Two types of volcanic activity have been recognised in the historical records of Mt. Etna: persistent activity from summit vents and periodic activity from eruptive fissures on the volcano's flanks (Guest and Murray 1979; Duncan et al. 1981; Acocella and Neri 2003; Behncke and Neri 2003; Branca and Del Carlo 2005; Crisci et al. 2010). Despite the typically explosive nature of summit

activity, its effects are often localised to within a few hundred/thousend meters of the eruption site and therefore its threat to property and surrounding populations is confined above 1600-1800 m above sea level; consequently, only the tourist facilities are potentially exposed to the risk of lava invasion (Duncan et al. 1981; Proietti et al. 2011; Cappello et al. 2013). However, flank eruptions tend to produce lava flows that can extend for far greater distances and lower elevations making them the greatest hazard on Mt. Etna (Duncan et al. 1981; Chester et al. 1985; Behncke and Neri 2003; Andronico and Lodato 2005; Behncke et al. 2005; Proietti et al. 2011). This greater relevance to lava flow hazard assessment, and the fact that the record of flank eruptions is considered reliable and nearly complete after 1600 AD (Mulargia et al. 1985; Behncke and Neri 2003; Branca and Del Carlo 2004; Behncke et al. 2005; Branca and Del Carlo 2005; Tanguy et al. 2007), whereas that of summit eruptions is only considered reliable after the late 19^{th} century (Chester et al. 1985; Andronico and Lodato 2005; Branca and Del Carlo 2005; Proietti et al. 2011), led us to exclude summit activity from this analysis and focus only on flank eruptions. Mt. Etna's flank eruptions occur from vents that are distributed unevenly across the volcano, being mostly concentrated in three rift zones and the Valle del Bove (Duncan et al. 1981; Acocella and Neri 2003; Behncke et al. 2005). Our compiled data includes information on vent location in order to investigate any relationships between duration and location.

Mt. Etna eruption duration data

The dataset used here contains flank eruptions from 1300 to 2010. It is a result of a critical examination of the catalogues and descriptions of summit and flank activity compiled by Tanguy (1981), Mulargia et al. (1985), Behncke and Neri (2003), Branca and Del Carlo (2004), Behncke et al. (2005), Branca and Del Carlo (2005), Tanguy et al. (2007) and Neri et al. (2011) and, in specific cases, additional information gleaned from other sources. For this study we are primarily interested in the duration of each flank eruption, so in those cases where flank activity occurred during a longer period of summit activity, the dates used are restricted to those of the flank component

only. For example, volcanic activity began from both summit and flank vents on the 18th May 1780. Summit activity continued into July (Tanguy et al., 2007), whereas the flank component of this eruption ended earlier, with reported end dates ranging from the 28th to the 31st May 1780 (Branca and Del Carlo 2004; Behncke et al. 2005; Branca and Del Carlo 2005; Tanguy et al. 2007). For this study the dates of the flank activity are used and this eruption is reported as starting on the 18th May and ending on the 29th May 1780. In a few other cases (e.g. May 1759), the precise dates of flank activity during times of summit activity are not reported. These flank eruptions have been excluded.

Some eruptions on Mt. Etna consist of more than one eruptive phase separated by periods of quiescence ranging from hours to days. An argument could be made that each phase constitutes a separate eruption, however, because some eruptions are described in detail whereas others are more vague it is unrealistic to assume that we have information about every quiescent period that occurred on Mt. Etna between the years 1300-2010. Instead we propose that periods of quiescence of less than 10 days between eruptive phases are not sufficient enough to warrant separating an eruptive sequence into two eruptions.

Accounting for Uncertainty

Uncertainties in the start and/or end dates of each eruption were considered in detail. One source of uncertainty is contradictory reporting. For example, the 1911 flank eruption is documented by Acocella and Neri (2003), Behncke and Neri (2003), Andronico and Lodato (2005), Behncke et al. (2005), and Neri et al. (2011) as starting on the 10th and ending on the 22nd September, and these dates were chosen as the preferred start and end dates of this eruption in this study. However, Mulargia et al. (1985) reported this eruption as starting one day earlier (9th September). To account for this an uncertainty in the duration of + 1 day has been assigned to the eruption's start date. Furthermore, Tanguy (1981) and Tanguy et al. (2007) reported this eruption as ending

one day earlier (21st September), whereas Branca and Del Carlo (2004) and Branca and Del Carlo (2005) reported it as ending one day later (23rd September). Here, an uncertainty in the duration of both + and - 1 day has been assigned to the eruption's end date. This results in a preferred eruption duration of 12 days (10th to 22nd September) with a maximum duration uncertainty of + 2 days (9th to 23rd September) and - 1 day (10th September to 21st September), thus the total duration of this eruption could range from 11 to 14 days. This method has been applied to all eruptions with contradictory start and/or end dates reported in the literature.

A second source of uncertainty arises where the start and/or end date of an eruption has been reported only to the nearest month or year. Here a date was assigned along with a number of days uncertainty, according to the method adopted by Bebbington and Lai (1996) and Benoit and McNutt (1996) (Table 1). Sometimes, despite an eruption's start or end only being known to the nearest month, slightly more qualitative information is provided indicating that it was 'early', 'mid' or 'late' in that month. Again the method of Benoit and McNutt (1996), summarised in Table 1 was applied.

[Table 1 about here]

Where all sources examined give the same start and end date for an eruption an uncertainty value is assigned based on whether the eruption is reported to the nearest day or whether hourly resolution is provided in the primary literature (Table 1).

Some eruptions carry both literature derived uncertainties and assigned uncertainties. For example, the 1755 eruption has a preferred duration of 6 days. This duration carries a + 1 day uncertainty which is derived from differences in the reported start date. The precise times of day that the eruption started and ended are unknown and although this literature derived uncertainty covers the potential for the eruption duration to have been slightly longer than 6 days, it does not allow for it to be slightly shorter. To account for this a - 0.5 day uncertainty in the eruption duration is assigned according to the 'nearest day' category of Table 1. The maximum uncertainty in the duration for

this eruption is therefore + 1 day and - 0.5 days.

80 known or suspected flank eruptions are reported from 1300 AD to 2010, however, 3 of these are excluded as their location is ambiguous and may be best described as summit eruptions (September 1869, February 1999 and July 2006). A further 11 eruptions have unknown durations (1333, August 1381, 1444, September 1446, September 1578/79, June 1607, March 1689, May 1759, 1764, July 1787, and November 1918) and 4 were excluded due to their duration uncertainty being greater than 50 % of their total preferred duration (November 1566, September 1682, August 1874 and December 1949). This results in 62 eruptions considered to have reliable durations that can be used in the following analyses (listed in Table 2) 49 of which carry duration uncertainties of less than +/- 10 %.

[Table 2 about here]

Additional information on specific eruptions

Tanguy et al. (2007) provide the most comprehensive catalogue of historical Etna eruptions extending from 1600 to 2003. The majority of the eruptions within this time period that are included in Table 2 are also reported by Tanguy et al. (2007), although sometimes, where numerous other sources give alternative dates, their dates are not used but are covered in the eruption's assigned uncertainty. Two eruptions, however, are not included by Tanguy et al. (2007). These are the February 1643 and the January eruptions (#8 and #41, Table 2). The latter eruption is documented in numerous other sources, including Tanguy (1981). It's exclusion by Tanguy et al. (2007) may have been an oversight, with other eruptions between 1966 and 1970 included in Tanguy (1981) but missing from Tanguy et al. (2007). The 1968 eruption is therefore included in our dataset using information from other sources (Table 2). The February 1643 eruption is excluded by Tanguy et al. (2007) due to some confusion in the literature between its vent location and the location of the 1646-7 lava flows (Tanguy et al., 2007), however we include this eruption here, using the dates

reported by Behncke et al. (2005) and Tanguy (1981).

Information about the dates of three other eruptions differ significantly from those recorded within the catalogue of Tanguy et al. (2007). These are the March 1956 and the February and November 1975 eruptions (#39, #45 and #46, Table 2). The flank eruption of March 1536 (#3, Table 2) was accompanied by summit activity that continued until the end of the year (Siebert et al. 2010; Tanguy et al. 2007). The flank component of this eruption is reported as ending in April (Behncke et al., 2005), whereas the information within appendix 1 of Tanguy et al. (2007) states that the eruption "probably ended on 8 April". To account for this uncertainty the precision to which the end date is known is considered to be in the 'early month' category of Table 1 so the 5th April is assigned with a +/- 5 day duration uncertainty (Table 2).

The two 1975 flank eruptions also occurred during a period dominated by summit activity. Such close association between the summit and flank activity makes isolating the dates of the flank component difficult and Tanguy et al. (2007) have simply recorded these eruptions within the longer summit activity. Other workers tried to resolve this, and it is the dates and uncertainty within these alternative references that are included in Table 2.

Mt. Etna vent location data

Flank eruptions at Mt. Etna are often the result of multiple aligned vents or fissures radiating from the volcano's summit (Acocella and Neri, 2003). Table 2 contains information about the location of each eruption. We have used 1:50,000 geological maps of Mt. Etna (Romano et al. 1979 and Branca et al. 2011) along with fissure maps within Chester et al. (1985) and Acocella and Neri (2003) to locate the source vents/fissures and lava flows for each eruption (Fig. 1).

The East flank of Mt. Etna is dominated by the large collapse feature of the Valle del Bove (Guest et al., 1984) and smaller Valle del Leone. The 19 eruptions with vents/fissures located within the

Valle del Bove and the 1 eruption within the Valle del Leone are identified as "VDB" or "VDL" in the location column of Table 2, however for the remainder of this paper the Valle del Leone eruption (#56, Table 2) will be grouped with the Valle del Bove eruptions and referred to as such.

[Fig. 1 about here]

The April 1971 eruption (#42 Table 2) was a complex flank eruption (Tanguy et al., 2007). The activity occurred at 3 vents on the upper south flank and a series of vents on the East flank of the volcano within the Valle del Bove and extending onto the NE flank (Branca and Del Carlo 2004; Branca and Del Carlo 2005; Tanguy et al. 2007; Le Guern 1972). Despite the varying location of activity during this eruption, and its association with the early formation of the summit's South-East crater, it is included here as one event with a duration of 68 days on the ENE flank.

The May 1879 and October 2002 eruptions (#27 and #59, Table 2) both involved more than one vent located on different flanks of the volcano. Here the vent which was active for each eruption's entire duration is used, although the erupted material from both vents are shown on the map in Fig. 1. Precise vent locations could not be found for two of the eruptions in Table 2 (#8 and #45), however examination of the literature and careful location of their erupted products has given enough evidence to assign approximate locations for these eruptions, with both eruptions #8 and #45 affecting the North-North-East region of the volcano.

The completeness of the historical record

The completeness of the eruption record requires some consideration when investigating past eruptive activity. It is important to recognise that some eruptions may have gone un-noticed or unrecorded entirely and that as a result our data (Table 2) is a sample of recorded eruptions only. The recording of Mt. Etna's eruptive activity dates back to Greek and Roman epochs (Branca and Del Carlo 2004; Branca and Del Carlo 2005; Tanguy et al. 2007). However, the records are often only

considered to be complete after 1600 AD (Mulargia et al. 1985; Behncke and Neri 2003; Branca and Del Carlo 2004; Behncke et al. 2005; Branca and Del Carlo 2005; Tanguy et al. 2007; Cappello et al. 2013). Fig. 2a shows an apparent increase in eruption frequency since 1300 AD which is most probably an artefact of reporting. Prior to 1600 data are scarce, and eruptions are often excluded due to insufficient information regarding their duration. Following 1600 AD the steepness of the curve increases and fewer eruptions are excluded due to the dataset becoming a complete representation of flank activity at Mt. Etna. All flank eruptions after 1970 have accurately known durations.

[Fig. 2 about here]

Fig. 2b shows that this increased reporting of eruptions with time is accompanied by an increase in the number of reported eruptions with short durations. This may suggest that the early eruption record is biased towards larger and more explosive eruptions, which would have made more of an impact on surrounding areas (Andronico and Lodato, 2005). This reporting bias appears to reduce during the 18th Century (Fig. 2b) and may reflect a shift towards more modern approaches in observing and documenting volcanic activity after the large 1669 flank eruption (Branca and Del Carlo 2004; Branca and Del Carlo 2005).

A regional bias in the quality and completeness of eruption records may also exist on Mt. Etna. The volcano's Western flank appears to have experienced fewer flank eruptions than other areas of the volcano (Fig. 1). Geological maps of Mt. Etna (Romano et al. 1979; Branca et al. 2011) show more lava flows on this flank than are represented in this study, however, these are either a result of eruptions prior to 1300 AD, and therefore outside the range of this investigation, or have undocumented eruption years. Although the reduced number of eruptions, especially in recent years, from vents located on Mt. Etna's West flank may reflect a preference for eruptive vents to open on other flanks, some of this may be a reporting bias due to the Western flank being the least populated region of Mt. Etna (Behncke et al., 2005). Similarly, 95 % of the reported eruptions

within the uninhabited and poorly accessible Valle del Bove post-date 1600 AD (Table 2), which may reflect a reporting bias here too.

Data before 1600 AD may be a poor representation of Mt. Etna's activity due to the reporting biases discussed and therefore cannot be used to make reliable forecasts about future activity. Data from before 1600 AD has therefore been excluded from the analyses in the remainder of this paper.

Statistical analysis

Survivor functions

The duration of a volcanic eruption can be considered as a type of survival time measurement. Survival analysis was first employed as a method of costing insurance premiums. It is now commonly used in medical studies to assess the length of remission following different treatments or in engineering situations to investigate the length of time before failure of an appliance or system (Machin et al., 2006). As with these types of data, eruption duration can be displayed graphically in an empirical survivor function plot, constructed by placing the observed durations (x_i) in rank order so that $x_1 \leq x_2 \leq \ldots \leq x_N$ where N is the total number of observations. The empirical survivor function ($\hat{F}(x_i)$) is then plotted at duration x_i where

$$\hat{F}(x_i) = \frac{N-i}{N}, \qquad i = 1, \ldots, N. \tag{1}$$

The resultant empirical survivor function curve provides information about the survival experience of that dataset. Typically these curves have an inverse 'S' shape with shallow distribution tails representing rarer events with unusually long or short durations and a steeper central portion where the majority of eruption durations plot. For example, Fig. 3 shows the empirical survivor function

curve for preferred eruption duration data between the years 1600 to 2010. It also displays curves for the maximum and minimum possible eruption durations, derived from individual eruption duration uncertainty (discussed previously and reported in Table 2). This plot demonstrates that the overall shape and position of the three empirical survivor function curves are very similar, implying that individual eruption duration uncertainty has a negligible effect on the overall distribution of the data.

[Fig. 3 about here]

Temporal variation in eruption duration

A fundamental assumption of any investigation using historical eruption data as an insight into future activity is that the character of past eruptions is a good indicator of the volcano's future activity (Chester et al. 1985; Behncke and Neri 2003; Behncke et al. 2005; Cappello et al. 2013). The following section considers the appropriateness of this assumption to the Mt. Etna data in Table 2.

At Mt. Etna, cycles of eruptive activity characterised by fluctuations in eruption frequency, type and output rate have been recognised on both century and decadal time scales (Wadge et al. 1975; Guest and Murray 1979; Behncke and Neri 2003; Allard et al. 2006; Smethurst et al. 2009; Cappello et al. 2013). Decade-scale cycles have been recognised at Mt Etna since 1865 with each cycle ending with a voluminous eruption, such as the flank eruptions of 1950-51 and 1991-93 (Behncke and Neri 2003; Allard et al. 2006; Cappello et al. 2013). The last century-scale cycle ended with the large 1669 eruption thus data recorded for eruptions between 1600 to 1670 represent activity during the culminating phase of a century-scale cycle (Behncke and Neri 2003; Tanguy et al. 2003; Cappello et al. 2013). During this time, erupted lavas were rich in plagioclase phenocrysts and believed to have been stored in a shallow magma reservoir within the volcanic edifice prior to

eruption. However, directly following the 1669 eruption Mt. Etna experienced a sharp decrease in productivity and a reduction in the phenocryst content of erupted lavas (Behncke and Neri, 2003). This has been attributed to the draining of a shallow magma reservoir within the volcanic edifice during the 17th Century (Hughes et al. 1990; Behncke and Neri 2003).

Previous studies have reported a general increase in eruption frequency with time that is not an artefact of reporting (Behncke and Neri 2003; Behncke et al. 2005; Branca and Del Carlo 2005; Cappello et al. 2013). In particular dramatic increases in eruption frequency and output rate have been recognised following 1971 (Andronico and Lodato 2005; Behncke et al. 2005; Branca and Del Carlo 2005; Smethurst et al. 2009; Cappello et al. 2013). A similar trend can be observed in our data (Table 2), with 20 eruptions in the past 39 years (1971-2010), as opposed to only 7 in the 41 years before it (1930-1971) (Fig. 2, Table 2). This is the equivalent of one third of the eruptions in this study having occurred in the most recent 5 % of the time period being investigated (1300-2010).

The distribution of eruption duration between 1600 and 1670 is dominated by long duration eruptions, three of which are longer than any subsequent eruption (Fig. 2b). It is possible that the shallow magma chamber exisiting at this time promoted longer duration eruptions. Since 1670 eruption durations range from 0.5 to 473 days. The increased frequency of eruptions following 1971 is accompanied by a reduction in short duration eruptions, with reported eruption durations of less than 6 days being absent after this time (Fig. 2b). Median eruption durations for these three time periods are 190 days (1600 to 1670), 24 days (1670-1971) and 50 days (1971-2010).

[Fig. 4 about here]

Fig. 4 shows empirical survivor function curves for the eruption durations of these three time periods. The 1670 to 1971 and 1971 to 2010 datasets show a divergence at durations less than 10 days (Fig. 4). If such variation in eruption duration distribution is significant, it could indicate a change in the dynamics of the volcanic system at c. 1971 in such a way that discourages short

duration eruptions, thus reducing their likelihood in the future. This implies that using the whole dataset of post-1670 eruptions would be an unrealistic representation of future activity, and that it might be more practical to use the 1971-2010 subset of the data. However a Mantel-Haenszel Logrank test (Appendix 1, and Machin et al. 2006) indicates that the curves are not statistically different at the 0.05 level and it cannot be concluded that they derive from different distributions (test statistic = 2 on 1 degree of freedom). For forecasting future eruption durations this implies that restricting the input data to eruptions from 1971-2010 is currently unnecessary.

In contrast, the empirical survivor function curve for the 1600-1670 dataset is offset from the 1670-1971 and 1971-2010 curves entirely (Fig. 4) and a Mantel-Haenszel Logrank test (Appendix 1, and Machin et al. 2006) indicates that this offset is statistically significant at the 0.05 level (test statistic = 7 and 5.3 on 1 degree of freedom, respectively). This clear difference and the evidence for a different plumbing system beneath Mt. Etna prior to 1670 may indicate that a future eruption of this scale and duration is unlikely and therefore that we should exclude this data from any forecasting models. However, recent investigations into the plumbing system of Mt. Etna indicate increasing magma accumulation beneath the volcano (Behncke and Neri 2003; Patané et al. 2003; Allard et al. 2006). This, along with the trend of increasing eruption frequency and output rate may indicate a gradual return to to the style of activity that was typical in the early 17th Century. By excluding this data the model is unable to account for the possibility that future activity at Mt. Etna could become more voluminous and potentially hazardous in the future (Behncke and Neri 2003; Patané et al. 2003; Allard et al. 2006).

Sectoral variation in eruption duration

Previous investigations into the location of historical flank eruptions at Mt. Etna have highlighted three regions of high vent density on the North-Eastern, Southern and Western flanks of the volcano. Three rift zones have been interpreted from the pattern of vent clustering within these regions and

have been identified as areas where eruptions are common (Duncan et al. 1981; Chester et al. 1985; Behncke et al. 2005; Neri et al. 2011; Proietti et al. 2011). To assess whether the distribution of eruption duration varies between each rift zone we have split the volcano into three sectors. Unlike Proietti et al. (2011) our sectors are not evenly distributed or positioned so that one boundary is directed North. Instead, we have used similar sectors to Behncke et al. (2005) whereby each sector contains one of the three identified rift zones along with any vents which appear closely associated with it. Using a point centred above the summit, these are between (A) 347^{o} and 104^{o}, (B) 104^{o} and 226^{o} and (C) 226^{o} and 347^{o} (Fig. 1), and include the North-Eastern, Southern and Western rift zones respectively.

The boundary between sectors A and B cuts through the Valle del Bove. Eruptions within this area are common and, since 1971, many lava flows from the summit's South East crater enter this valley making the resurfacing rate high such that identifying vents and fissures within this area can be difficult. The precise positions of the 1955 and 1802 fissures (#13 and #19, Table 2) are unknown, but reported to be close to Rocca Mussarra and are therefore considered here as part of sector A. Other fissures and vents within the Valle del Bove have been located using the sources previously discussed and assigned to sector A or B accordingly.

The majority of eruptive vents and fissure outside of the Valle del Bove fall clearly within one of the three sectors (Fig. 1). The March 1981 eruption (#51, Table 2) was the result of a long fissure which crosses the boundary between sectors A and C. The eruption is most probably a result of the North-East rift zone and is therefore considered part of sector A (Fig. 1). Similarly the eruptive fissure of the May 2008 eruption (#62, Table 2) crosses the boundary between sectors A and B. The lower portion of this fissure was active throughout the eruption and thus the eruption is attributed here to sector B (Fig. 1).

[Fig. 5 about here]

Empirical survivor function curves plotted for the 1600 to 2010 eruptions in sectors A, B and C are

displayed in Fig. 5. To assess whether such differences are significant, Mantel-Haenszel Logrank tests have been performed on all possible combinations of sector pairs (i.e. A-B, A-C and B-C) and the results are summarised in Table 3. Despite the median duration of Sector B (84 days) being higher than that for sectors A and C (18 days and 19.5 days respectively) results indicate that the curves cannot be considered statistically different at the 0.05 level.

[Table 3 about here]

Forecasting the duration of future flank eruptions

Description of the statistical model

When duration data are modelled using theoretical distributions, survival analysis can be used to estimate the probability that a future eruption will exceed a given length of time. The probabilistic forecasts are based on best-fit parametric statistical models of empirical survivor functions. The two parameter log-logistic and the three parameter Burr type XII distributions have been considered and their survivor functions are shown in equation 2.

$$\hat{F}(x)_{\,(Log-logistic)} = \frac{1}{1+(x/\sigma)^{\beta}}$$
$$\hat{F}(x)_{\,(Burr\,XII)} = \frac{1}{\{1+(x/\sigma)^{\beta}\}^{\alpha/\beta}} \tag{2}$$

To identify the best-fit log-logistic and Burr type XII survivor functions their parameters (α, β and σ) have been found by maximum likelihood estimation and their goodness of fit to the observed

duration data tested using a Kolmogorov-Smirnov test. If the Kolmogorov-Smirnov results indicate that the observed duration data could have been derived from either distribution, a chi-squared test is used to assess whether there is any benefit in employing the more complicated Burr type XII distribution or whether the simpler log-logistic distribution provides an equally good fit to the data. Additional information on these methods can be found in Appendix 2.

The modelled best-fit survivor function can be used to make probabilistic forecasts about the duration of future and on-going volcanic eruptions. Three types of forecast are made in this investigation. The first is the probability of exceeding a specified duration x according to the survivor function given in equation 2. The second is a variation on the survivor function, adapted for on-going eruptions. The residual life function is used to find the probability of exceeding a specified total duration x, having already reached duration t and is given by

$$\hat{F}_t(x)_{\,(Log-logistic)} = \frac{\sigma^\beta + t^\beta}{\sigma^\beta + x^\beta}$$
$$\hat{F}_t(x)_{\,(Burr\,XII)} = \left(\frac{\sigma^\beta + t^\beta}{\alpha^\beta + x^\beta}\right)^{\alpha/\beta} \tag{3}$$

Finally, the quantile function given by

$$x_{p\,(Log-logistic)} = \sigma\left(\frac{p}{1-p}\right)^{1/\beta}$$
$$x_{p\,(Burr\,XII)} = \sigma\left\{\frac{1}{(1-p)^{\beta/\alpha}} - 1\right\}^{1/\beta} \tag{4}$$

enables the user to find the duration associated with a stated quantile p, that is, the duration that has probability $1 - p$ of being exceeded. For each forecast the 95 % and 80 % confidence intervals have been calculated using the method discussed in Appendix 3.

Application of the model to Mt. Etna

The above investigations have shown that differences in the distribution of eruption duration before and after 1971 and differences in the distribution of eruption duration on different sectors of Mt. Etna's flanks are not statistically significant. This indicates that the eruption durations recorded between 1670 and 2010 could have all derived from the same distribution, and therefore it is acceptable to use all the available data in the forecasting model presented below. We have also demonstrated that the distribution of eruption duration between 1600 and 1670 is dominated by long duration eruptions which may be a result of a shallow magma reservoir existing beneath Mt. Etna at this time. We have made eruption duration forecasts on two different datasets; including and excluding these data (1600-2010 and 1670-2010 respectively). The 1600-2010 dataset allows us to account for all possible future activity including eruption durations expected in the culminating phase of a century-scale cycle. It contains a total of 58 observed eruption durations ranging from less than 1 day to 3653 days with a median duration of 34.5 days (Table 2). The 1670-2010 dataset may give a more realistic forecast of eruption durations in the near future i.e. before the culminating phase of the current century-scale cycle. This dataset contains 51 observed eruption durations ranging from less than 1 day to 473 days with a median duration of 26 days (Table 2).

For both the 1600-2010 and 1670-2010 datasets the Kolmogorov-Smirnov goodness of fit test suggests that the observed durations could have been derived from either a log-logistic or Burr type XII distribution. Additional chi-squared tests indicate that there is no benefit in applying the Burr type XII distribution over the log-logistic distribution. The best fit log-logistic survivor functions have estimated parameter values of 0.94 and 40.56 (1600-1670) and 1.00 and 33.00 (1670-2010) for

409 β and σ respectively. The resultant survivor function curves are displayed graphically along-side
410 their empirical survivor curves (Emp_SF) in Fig. 6.

411 [Fig. 6 about here]

412 Table 4 contains the results of seven forecasts made from the 1600-2010 and 1670-2010 datasets;
413 three using the survivor function (Tables 4a and 4b), two using the residual life function where t
414 is 14 days (Tables 4c and 4d) and two using the quantile function (Tables 4e and 4f). The values
415 displayed in the first column of each table represents the scenario being forecast, i.e. the probability
416 of an eruption exceeding 7 days or the duration associated with a p value of 0.34. The final two
417 columns in each table represent the 95 % and 80 % confidence intervals that have been calculated.
418 When discussed in the text 80 % confidence intervals are quoted.

419 [Table 4 about here]

420 The shape and position of the two empirical survivor function curves in Fig. 6 are similar. The
421 greatest difference is the prominent long duration tail of the empirical survivor function curve in
422 Fig. 6a (1600-2010) which is absent in Fig. 6b (1670-2010). This is a result of the long duration
423 eruptions which occurred between 1600 and 1670. The effect of this on the forecasting model
424 results is that the probability of exceeding a given duration is consistently lower for the 1670-2010
425 dataset than the 1600-2010 dataset and that this difference is slightly greater when forecasting
426 longer duration eruptions (Table 4). For example, when the 1600-2010 dataset is considered, results
427 show an 84 % ($\pm$ 5 %) probability of exceeding 1 week (7 days) and a 57 % ($\pm$ 7 %) probability of
428 exceeding 1 month (30 days). These probabilities are reduced by 2 % and 5 % respectively, when
429 the 1670-2010 dataset is considered (Tables 4a and 4b). A similar trend is also present in the results
430 of the residual life function (Tables 4c and 4d).

431 The survivor function and residual life function both give the probability of exceeding stated dura-
432 tions. Perhaps more useful is the quantile function, allowing the user to identify durations associ-

ated with specific probabilities. Furthermore, the assignment of qualitative terms such as 'likely' and 'unlikely' to sensible probabilities make the model results accessible to a wider audience. Here we consider a 'likely' result as having a probability of 66 % or more, and an 'unlikely' result as having a probability of 33 % or less (Budescu et al. 2009; Mastrandrea et al. 2010). These equate to p values of 0.34 and 0.67 respectively. The results of such forecasts are shown in Tables 4e and 4d. Using the 1600-2010 dataset results show a 66 % probability of exceeding 20 days ($\pm$ 7 days) and a 33 % probability of exceeding 86 days ($\pm$ 29 days) (Table 4e), therefore it can be concluded that a future flank eruption on Mt. Etna is likely to exceed 20 days but unlikely to exceed 86 days. When the dataset is restricted to post 1670 eruptions, thus excluding the activity which occurred in the culminating phase of the last century-scale cycle these durations are reduced to 17 days ($\pm$ 6 days) and 67 days ($\pm$ 22 days), respectively (Table 4f).

Conclusions

We have introduced a probabilistic model forecasting the duration of future and on-going eruptions using a new dataset of historical flank eruption durations from Mt. Etna. The model shows great potential for future use as a forecasting tool and could greatly benefit emergency response planning both prior to and during volcanic crises. It is not specific to Mt. Etna and can easily be adapted for use on other highly active, well documented volcanoes or for different duration data such as the duration of explosive episodes or the duration of repose periods between eruptions. The model uses datasets of historical eruption durations and thus relies on past eruptions being a good indicator of future activity. It is therefore limited to use on volcanoes with well documented historic eruptions and data must firstly be assessed for reporting biases and any changes in eruption duration with time or location.

Critical assessment of documented flank eruptions from Mt. Etna resulted in a reliable dataset of reported eruption durations between the years 1600 and 2010 containing 58 eruptions with reported

durations ranging from less than 1 day to 3653 days. Eruptions between the years 1600 and 1670 include the three longest duration flank eruptions reported at Mt. Etna. As a result this time period is statistically different from that following 1670. Although usually this would be cause to exclude this data, the 1600 to 1670 time period represents the culminating phase of a century long cycle and a return to eruptions of this scale and duration in the future is conceivable. Other temporal variations in eruption duration were assessed but not been found to be statistically significant. Furthermore, significant difference in the distribution of eruption duration from the prevailing three rift zones on Mt Etna (NE, S and W) were also not found.

We chose to run the forecasting model on two datasets; 1600-2010 and 1670-2010, allowing us to asses the effect of including the longer duration 1600-1670 eruptions. Results indicate that the probability of exceeding a given duration is consistently less for the 1670-2010 dataset, however, the degree to which this is the case is slight, especially where short durations are involved. When using the 1600-2010 dataset of historical flank eruption durations and by assigning the terms 'likely' and 'unlikely' to probabilities of 66 % and 34 % respectively, the forecasting model was used to indicate that a future flank eruption on Mt. Etna would be likely to exceed 20 days (+/- 7 days) and unlikely to exceed 86 days (+ 29 days).

Acknowledgements

LSG is supported by a Natural Environment Research Council PhD studentship. We thank John Murray for his invaluable knowledge of Mt. Etna's volcanic activity and historical eruptions and Peter Fawdon for his use of Arc GIS to obtain bearings of vent locations.

Appendices

Appendix 1: Mantel-Haenszel Logrank test for comparing empirical survivor functions

A Logrank test has been used to assess the significance of any differences between the empirical survivor functions of two groups of duration data (g_1 and g_2). The method and equations outlined below are based on the information within Machin et al. (2006).

Firstly the observed durations (x) are placed in rank order irrespective of their original group and the expected number of eruptions ending from each group is then estimated at each duration interval (i) using

$$E_{\{g_1,i\}} = \frac{r_i T_{\{g_1,i\}}}{N_i} \qquad and \qquad E_{\{g_2,i\}} = \frac{r_i T_{\{g_2,i\}}}{N_i}. \tag{5}$$

Here r_i is the total number of observed eruptions with duration i (irrespective of group), T_i is the total number of eruptions in the specified group (g_1 or g_2) with durations longer than or equal to i and N_i is the total number of observations in both groups with durations longer than or equal to i. The total number of observations in each group (O_{g_1} and O_{g_2}) and the total expected number of eruptions ending in each group (E_{g_1} and E_{g_1}) are calculated. For better treatment of tied data, where two or more observed eruptions are of equal duration, the Mantel-Haenszel version of the Logrank test is employed, involving the calculation of the hypergeometric variance V at each duration interval:

$$V_i = \frac{T_{\{g_1,i\}} T_{\{g_2,i\}} r_i s_i}{N_i^2 (N_i - 1)} \tag{6}$$

where s_i is the total number of observed eruptions with durations longer than i (irrespective of group). The χ^2_{MH} Logrank statistic is calculated by either:

$$\chi^2_{MH} = \frac{(O_{g_1} - E_{g_1})^2}{V} \qquad or \qquad \chi^2_{MH} = \frac{(O_{g_2} - E_{g_2})^2}{V} \tag{7}$$

The null hypothesis of the log-rank test is that the datasets being compared all have the same survival experience, and thus any variation between their empirical survivor functions can be attributed purely to chance (Machin et al., 2006). The resultant test statistic is compared to the 95 % χ^2 distribution quantile with degrees-of-freedom equal to one less than the number of groups being compared, and the null hypothesis is rejected if the test statistic is larger than this quantile.

A variation of this test can be used to compare three or more empirical survivor functions allowing the user to establish whether the differences are statistically significant, however, it does not provide information about where these differences occur. For this reason, we have chosen not to use this modified test, but to run the Logrank test outlined above on pairs of empirical survivor functions to assess where significant differences lie.

Appendix 2: Modelling using appropriate statistical distributions

In order to make probabilistic forecasts of future eruption durations empirical survivor function curves are modelled using a theoretical distribution. The log-logistic and Burr type XII distributions are tested in this study, and the survivor functions and related equations are shown in equations 2, 3 and 4, where x is duration, σ a scale parameter and both α and β are shape parameters. In both distributions the duration is the only known quantity and all parameters have been estimated using maximum likelihood. Early stages of this investigation also tested the fit of exponential and Weibull distributions, however, these have provided insufficient fits to all duration datasets studied.

A Kolmogorov-Smirnov (KS) goodness of fit test has been used to determine whether the distributions provide a good fit to the observed duration data. This test is based on comparisons between the empirical distribution function (F_n) of the observed data and the cumulative distribution function (F_0) of an assumed theoretical distribution. These equate to the inverse of the empirical survivor function (Equation 1) or theoretical distribution's survivor function (equation 2), respectively. Graphically, the KS test statistic D identifies the maximum vertical displacement between F_n and F_0 and thus is obtained by computing the maximum absolute difference between F_n and F_0 at all values of x:

$$D = \underset{x}{Max}|F_n(x) - F_0(x)| \tag{8}$$

The null hypothesis of this test is that the observed sample can be said to have derived from the theoretical distribution being tested. It can be accepted when the KS statistic is lower than the critical value for that sample size (N) and appropriate significance level. Here we test at a 5 % significance level where the critical value is given by $\frac{1.36}{\sqrt{N}}$.

Some degree of approximation has been introduced to this method due to the parameters of the theoretical distributions being estimated from the observed duration data and the presence of tied data in the low duration region of the dataset. These are considered to have a negligible effect on the final test result.

Where both distributions satisfy the criteria to accept the null hypothesis a further test is used to determine whether it is worthwhile applying the more complex Burr type XII distribution or whether the simpler Log-logistic distribution provides an adequate fit to the data. To determine this the difference between the maximised values of the log-likelihood associated with each distribution is doubled, and the resultant value compared to the χ^2 distribution quantile on 1 degree-of-freedom at the 5 % significance level (3.84). If the calculated value is greater than this critical value, then

the null hypothesis, that there is no difference between the two distributions is rejected and the Burr type XII distribution is used to model the observed duration data.

Appendix 3: Calculating 95 % and 80 % confidence intervals on model results

The results of the forecasting models presented so far are 'point estimates' for the specific value of interest (x or p for the survivor/residual life function and quantile function models, respectively). In each case 95 % and 80 % confidence intervals are given in the form of

$$'point\,estimate' \quad +/- \quad 1.96\,\sqrt{\hat{V}}$$

and

$$'point\,estimate' \quad +/- \quad 1.28\,\sqrt{\hat{V}}$$

respectively, where $\hat{V}$ is the estimated variance for the formula being used in the model. The calculation of $\hat{V}$ is specific to the theoretical distribution and and is based on standard asymptotic theory for maximum likelihood estimation. The equations involved are displayed in Table 5. There, the C's are elements of the asymptotic covariance matrix associated with the maximum likelihood estimates $\hat{\beta}$ and $\hat{\sigma}$ of β and σ, respectively.; specifically, C[1,1] is the asymptotic variance of $\hat{\beta}$, C[2,2] that of $\hat{\sigma}$ and C[1,2] is the asymptotic covariance between $\hat{\beta}$ and $\hat{\sigma}$.

[Table 5 about here]

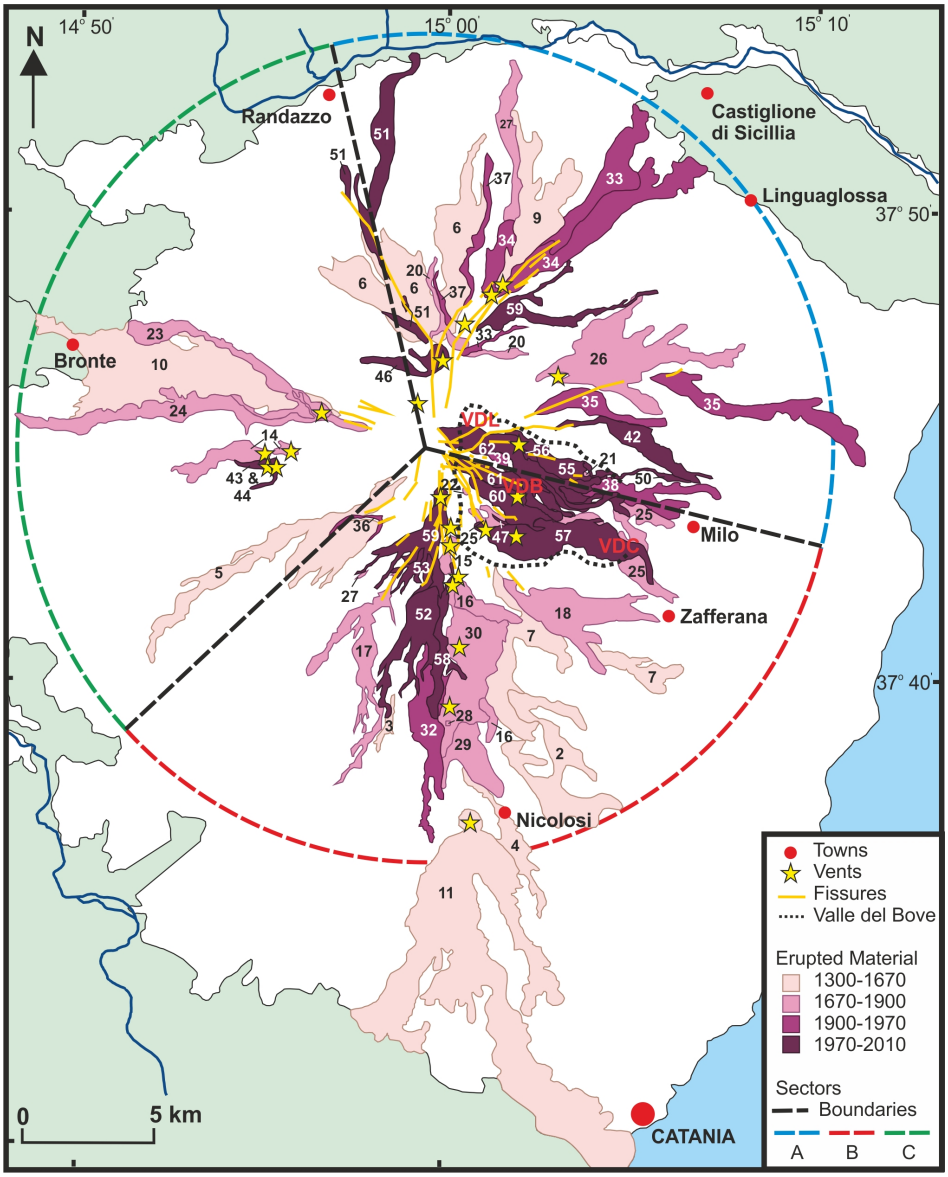

Figure 1: Sketch map of Mt. Etna based on Romano et al. (1979) and Branca et al. (2011) showing the extent of erupted material and the position of their vents/fissures (stars/ yellow lines) for the eruptions within Table 2. Dashed lines represent the boundaries between sectors A, B and C (discussed in the text), VDB = Valle del Bove, VDL = Valle del Leone and VDC = Valle del Calanna

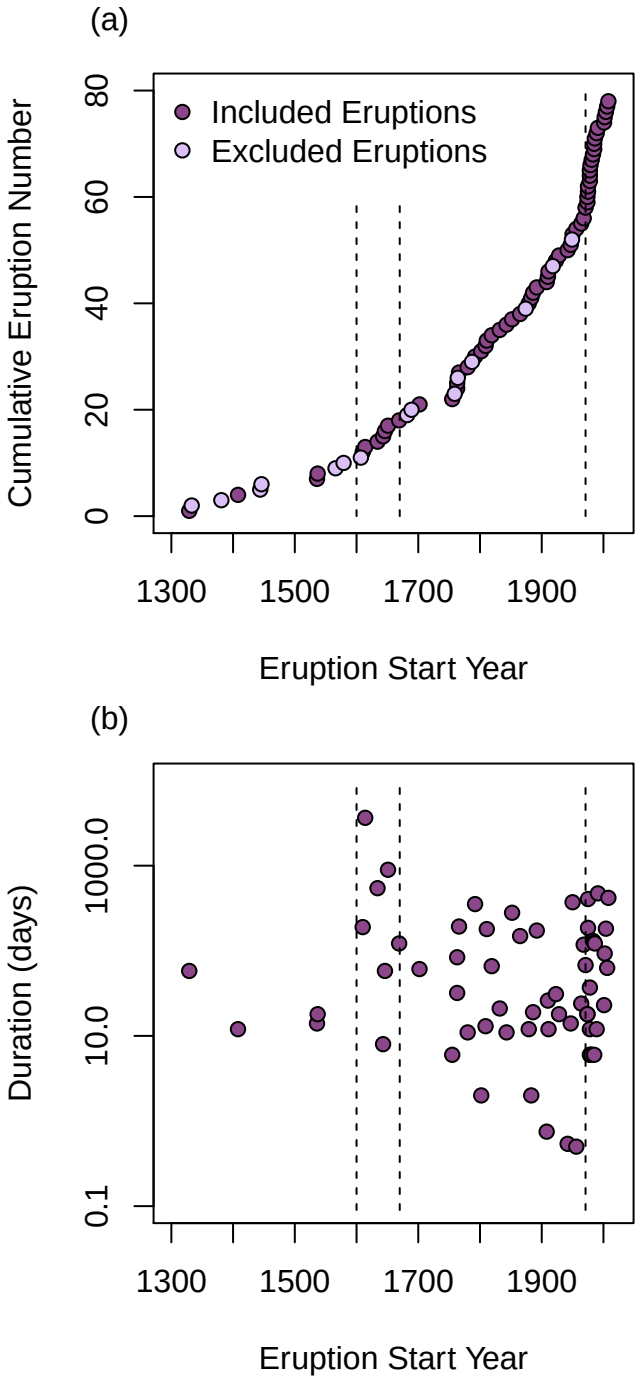

Figure 2: (a) Plot of cumulative eruption number against eruption start year of all 77 flank eruptions reported between 1300 and 2010. Pale symbols represent the 15 eruptions excluded from this study due to insufficient information regarding their start and/or end date. (b) Plot of eruption duration (on a log scale) against start year for the 62 eruptions included in this study (Table 2). Vertical dashed lines in both plots represent the years 1600, 1670 and 1971

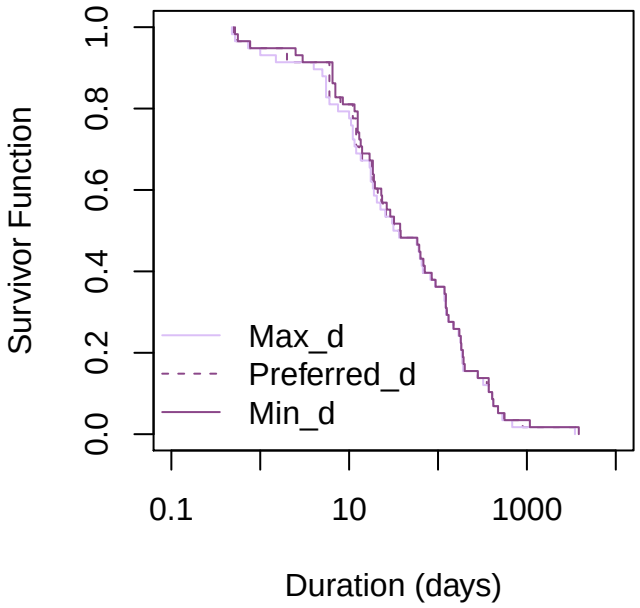

Figure 3: Empirical survivor function curves for preferred eruption durations from 1600-2010 along with curves for their maximum and minimum possible eruption durations when uncertainty is taken into account (data from Table 2)

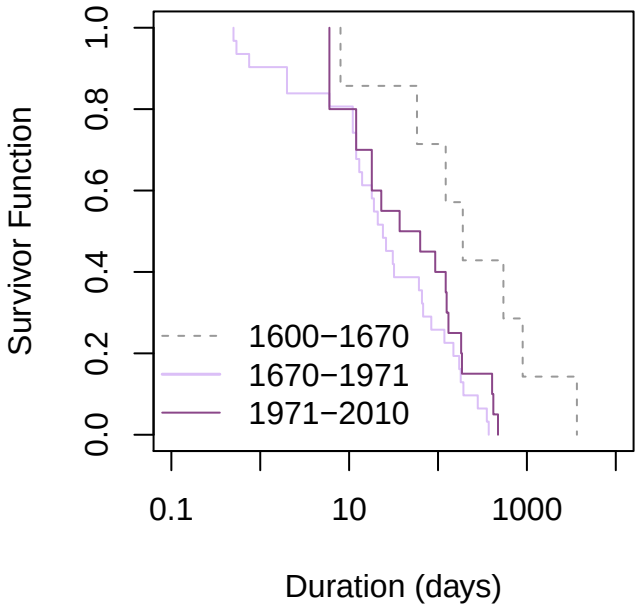

Figure 4: Empirical survivor function curves for eruption durations from 1600-1670 ($n = 7$), 1670-1971 ($n = 31$) and from 1971-2010 ($n = 21$) (data from Table 2)

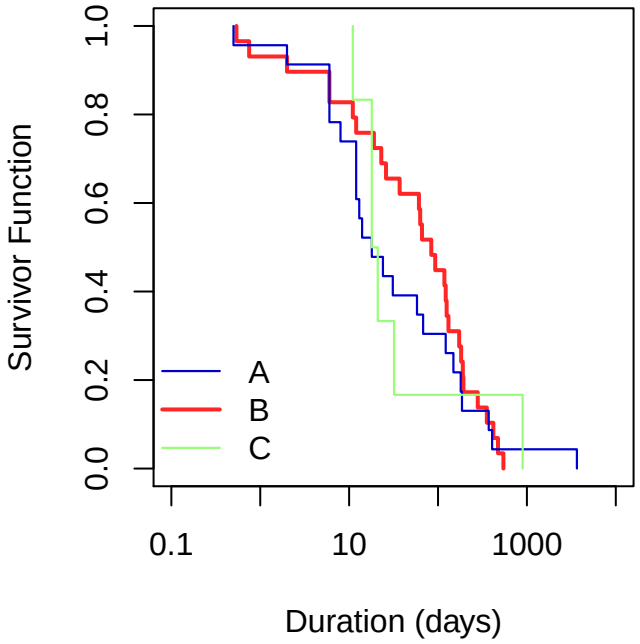

Figure 5: Empirical survivor function curves for eruption durations within sectors A ($n = 23$), B ($n = 29$) and C ($n = 6$) between the years 1600 and 2010 (data from Table 2)

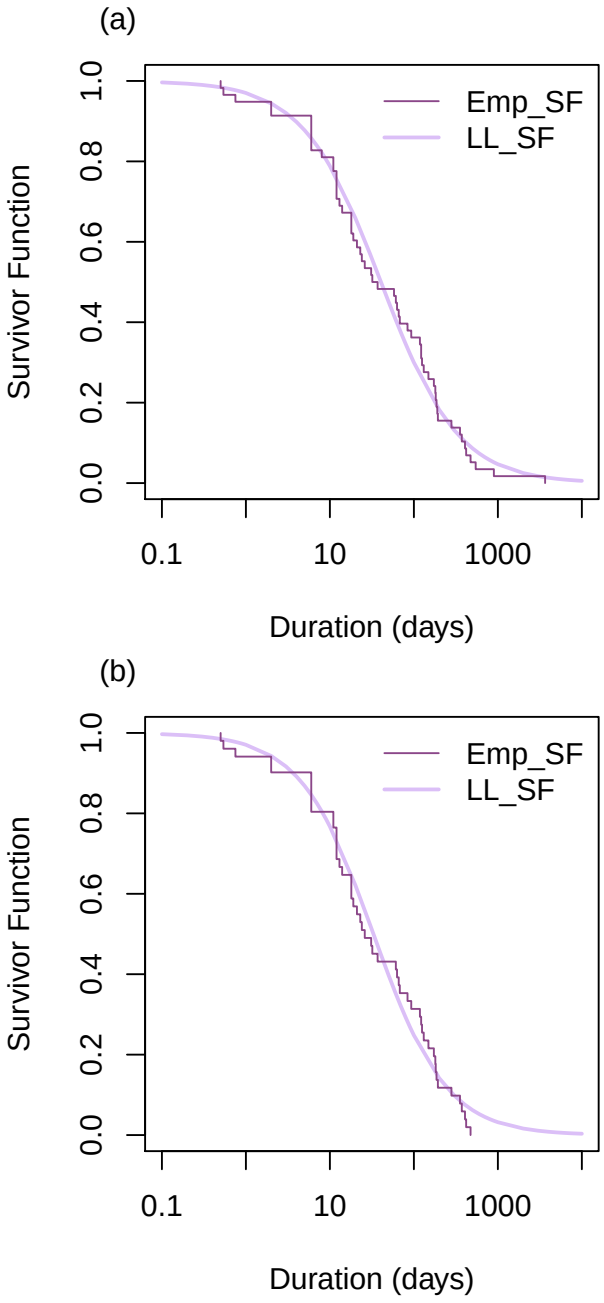

Figure 6: Empirical survivor function (Emp_SF) curves along with their best-fit log-logistic survivor function curves for historical flank eruption durations at Mt Etna (data from Table 2) from (a) 1600-2010 (β = 0.94, σ = 40.56) and (b) 1670-2010 (β = 1.00, σ = 33.00)

Table 1: Table of assigned dates and uncertainties

Reporting	**Date**	**Uncertainty (days)**	**Example**
Nearest hour	-	+/- 0.02	June 1942
Nearest day	-	+/- 0.5	Jan 1865
Nearest month	15/mm/yyyy	+/- 15	Dec 1636 (end)
Nearest year	01/07/yyyy	+/- 182.5	July 1614 (end)
'*Early*' month	05/mm/yyyy	+/- 5	March 1536 (end)
'*Mid*' month	15/mm/yyyy	+/- 5	-
'*Late*' month	25/mm/yyyy	+/- 5	-

mm = Reported month, *yyyy* = Reported year

Table 2: Dataset of historical Etna flank eruptions with known durations, 1300-2010

#	Location		Preferred start date	reference	Preferred end date	reference	Preferred duration (days)	Duration U/C (days) Start	End	Max
1	VDB		28/06/1329	[1,2,3]	25/08/1329	[1,2]	58		*+5* *-5*	*+5* *-5*
2	S-Rift		09/11/1408	[1,2,3]	21/11/1408	[3]	12			*+0.5* *-0.5*
3	S-Rift		22/03/1536	[1,2,3]	05/04/1536	[1,2,3]	17		*+5*	*+5*
4	S-Rift		11/05/1537	[3]	29/05/1537	[3]	18	+1 -1	*-5*	*-5* +1 -1
5	SW flank	(B)	06/02/1610	[1,2,3,4,5]	15/08/1610	[1,2,5]	190			*+0.5* *-0.5*
6	NE-Rift	(A)	01/07/1614	[1,2,3,5]	01/07/1624	[1,2,3,5]	3653		*+182.5* *-182.5*	*+182.5* *-182.5*
7	S-Rift	(B)	19/12/1634	[2,3,4,5]	15/06/1636	[1,2,3]	544	+1	*+15* *-15*	+16 -15
8	NE-flank	(A)	20/02/1643	[2,5]	28/02/1643	[2,5]	8			*+0.5* *-0.5*

Continued on next page...

Table 2 – Continued

#	Location		Preferred start date	reference	Preferred end date	reference	Preferred duration (days)	Duration U/C (days) Start	End	Max
9	NE-Rift	(A)	20/11/1646	[1,2,3,4,5]	17/01/1647	[1,2,3,4,5]	58			*+0.5* *-0.5*
10	W-Rift	(C)	17/01/1651	[1,2,3]	01/07/1653	[1,2,3]	896	+1 -30	*+182.5* *-182.5*	+183.5 -212.5
11	S-Rift	(B)	11/03/1669	[1,2,3,4,5]	11/07/1669	[1,2,3,4,5]	122			*+0.5* *-0.5*
12	VDB	(B)	08/03/1702	[1,2,3,4,5,6]	08/05/1702	[1,2,3,5,6]	61			*+0.5* *-0.5*
13	VDB	(A)	09/03/1755	[2,3,4,5,6]	15/03/1755	[1,2,3,4,5,6]	6	+1		+1 *-0.5*
14	W-Rift	(C)	06/02/1763	[1,2,3,4,5,6]	10/03/1763	[3,5,6]	32	+1	+5	+6 *-0.5*
15	S-Rift	(B)	18/06/1763	[2,3,5,6]	10/09/1763	[1,2,3,5,6]	84	+1 -2		+1 -2
16	S-Rift	(B)	28/04/1766	[1,2]	07/11/1766	[1,2]	193	+1	-1	+1 -1
17	S-Rift	(B)	18/05/1780	[1,2,3,4,5]	29/05/1780	[3]	11		+2 -1	+2 -1

Continued on next page...

Table 2 – Continued

#	Location		Preferred start date	reference	Preferred end date	reference	Preferred duration (days)	Duration U/C (days) Start	End	Max
18	S-Rift	(B)	26/05/1792	[3,5,6]	15/05/1793	[1,2,3,5,6]	349	+3 -17	*+15* *-15*	+18 -32
19	VDB	(A)	15/11/1802	[1,2,3,4,5,6]	17/11/1802	[2]	2		*+1* -1	+1 -1
20	NE-Rift	(A)	27/03/1809	[1,2,3,5,6,7]	09/04/1809	[1,2,5,6,7]	13	-1		*+0.5* -1
21	VDB	(A)	27/10/1811	[1,2,3,5,6]	24/04/1812	[1,2,3,5,6]	180	-1		*+0.5* -1
22	VDB	(B)	27/05/1819	[1,2,3,4,5,6]	01/08/1819	[1,2]	66	+1	+4	+5 *-0.5*
23	W-Rift	(C)	01/11/1832	[1,2,4]	22/11/1832	[1,2,3,5,6]	21	+2		+2 *-0.5*
24	W-Rift	(C)	17/11/1843	[1,2,3,4,5,6,7]	28/11/1843	[1,2,3,5,6,7]	11			*+0.5* *-0.5*
25	VDB	(B)	20/08/1852	[1,2,3,4,5,6,7]	27/05/1853	[1,2,3,5,6,7]	280			*+0.5* *-0.5*
26	NE flank	(A)	30/01/1865	[1,2,3,5,6,7]	28/06/1865	[1,2,3,5,6]	149			*+0.5* *-0.5*

Continued on next page...

Table 2 – Continued

#	Location		Preferred start date	reference	Preferred end date	reference	Preferred duration (days)	Duration U/C (days) Start	End	Max
27	NE-Rift	(A)	26/05/1879	1,2,3,5,6,7	07/06/1879	1,3,5,6,7	12		-1	*+0.5* -1
28	S-Rift	(B)	22/03/1883	1,2,3,4,5,6,7	24/03/1883	1,2,3,5,6	2			*+0.5* *-0.5*
29	S-Rift	(B)	19/05/1886	2,3,5,6,7	07/06/1886	1,2,3,5,6,7,8	19			*+0.5* *-0.5*
30	S-Rift	(B)	09/07/1892	1,2,3,5,6,7,8	29/12/1892	1,2,3,5,6,8	173	-2	-1	*+0.5* -3
31	VDB	(B)	29/04/1908	1,2,3,4,5,6,8,9,10,11	30/04/1908	1,2,3,5,6,8,9,10,11	0.75			*+0.02* *-0.02*
32	S-Rift	(B)	23/03/1910	1,2,3,4,5,6,7,8,9,10,11	18/04/1910	1,2,3,5,6,7,8,9,10,11	26			*+0.5* *-0.5*
33	NE-Rift	(A)	10/09/1911	1,2,3,5,6,7,8,9,10,11	22/09/1911	2,5,9,10,11	12	+1	+1 -1	+2 -1
34	NE-Rift	(A)	17/06/1923	1,2,3,5,6,7,8,9,10,11	18/07/1923	1,2,3,5,6,7 8,9,10,11	31	+1		+1 *-0.5*

Continued on next page. . .

Table 2 – Continued

#	Location		Preferred start date	reference	Preferred end date	reference	Preferred duration (days)	Duration U/C (days) Start	End	Max
35	NE flank	(A)	02/11/1928	1,2,3,5,6,8, 9,10,11,12	20/11/1928	1,2,3,5,6,8, 9,10,11,12	18	-1		*+0.5* -1
36	SW flank	(B)	30/06/1942	1,2,3,4,5,6, 8,9,10,11	30/06/1942	1,2,6,9,10	0.54			*+0.02* *-0.02*
37	NE-Rift	(A)	24/02/1947	1,2,3,5,6,8, 9,10,11	10/03/1947	1,2,3,5,6,8, 9,10,11	14	+3		+3 *-0.5*
38	VDB	(A)	25/11/1950	1,2,3,4,5,6, 8,9,10,11	02/12/1951	1,2,3,6,8	372		-1	*+0.5* -1
39	VDB	(A)	01/03/1956	2,3,6,9	02/03/1956	2,3,6,9	0.5			*+0.02* *-0.02*
40	VDB	(A)	01/02/1964	2,3,6	25/02/1964	2,3,6	24		*+5* *-5*	*+5* *-5*
41	VDB	(B)	07/01/1968	2,3,5,6,9,10,	04/05/1968	2,3,5,6,9,11	118			*+0.5* *-0.5*
42	E flank	(A)	05/04/1971	1,2,3,5,6,8,9,10 11,13,14,15,16	12/06/1971	1,2,3,5,6,8,9 10,11,13,14,15	68			*+0.5* *-0.5*
43	W-Rift	(C)	30/01/1974	1,2,3,4,5,6, 9,10,11,17	17/02/1974	1,2,5,9,10,11, 17	18		+1	+1 *-0.5*

Continued on next page...

Table 2 – Continued

#	Location		Preferred start date	reference	Preferred end date	reference	Preferred duration (days)	Duration U/C (days) Start	End	Max
44	W-Rift	(C)	11/03/1974	1,2,3,4,5,6,9,10,11,17	29/03/1974	1,2,3,5,6,9,10,11,17	18			+0.5 -0.5
45	NE-Rift	(A)	24/02/1975	2,3,5,6,9,10,11,18	29/08/1975	3,5,6,9,10,11	186		+14	+14 -0.5
46	NW flank	(A)	29/11/1975	2,3,5,6,9,10,11	08/01/1977	3,5,6,8,10,11	406			+0.5 -0.5
47	VDB	(B)	29/04/1978	1,2,3,4,5,6,8,9,10,11	05/06/1978	1,3,5,6,8,9,10,11	37			+0.5 -0.5
48	VDB	(B)	24/08/1978	3,4,6,8	30/08/1978	3,5,6,8,9,10,11	6	+1 -1	-1	+1 -2
49	VDB	(B)	18/11/1978	3,4,6,8	30/11/1978	3,5,6,9,10,11	12	-5	-1	+0.5 -6
50	VDB	(A)	03/08/1979	1,2,3,5,6,8,9,10,11	09/08/1979	1,2,3,5,6,8,9,10,11	6			+0.5 -0.5
51	N flank	(A)	17/03/1981	1,3,5,6,8,9,10,11	23/03/1981	3,5,6,8,9,10,11	6		-1	+0.5 -1
52	S-Rift	(B)	28/03/1983	1,3,5,6,8,9,10,11	06/08/1983	1,3,5,6,8,9,10,11	131			+0.5 -0.5

Continued on next page...

Table 2 – Continued

#	Location		Preferred start date	reference	Preferred end date	reference	Preferred duration (days)	Duration U/C (days) Start	End	Max
53	S-Rift	(B)	10/03/1985	1,5,9,10,11	13/07/1985	1,3,5,6,9,10, 11	125	-2		+0.5 -2
54	VDB	(A)	25/12/1985	1,5,6,9,10,11, 19	31/12/1985	1,5,6,9,10,11, 19	6			+0.5 -0.5
55	VDB	(A)	30/10/1986	1,3,5,6,8,9,10 11	01/03/1987	3,5,6,9,10,11	122		-4	+0.5 -4
56	VDL	(A)	27/09/1989	1,3,5,6,8,11	09/10/1989	1,3,5,6,8,9, 10,11	12			+0.5 -0.5
57	VDB	(B)	14/12/1991	1,3,9,5,6,8, 10,11	31/03/1993	1,3,5,6,9,10, 11	473		-1	+0.5 -1
58	S-Rift	(B)	17/07/2001	1,3,6,10,11,19, 20,21	09/08/2001	1,3,6,10,11,19, 20,21	23			+0.5 -0.5
59	S-Rift	(B)	27/10/2002	1,3,5,6,11	28/01/2003	1,3,5,6,11	93	+1		+1 -0.5
60	SE flank	(B)	07/09/2004	5,11,21,22,23	08/03/2005	5,11,23	182			+0.5 -0.5
61	E flank	(B)	12/10/2006	24	14/12/2006	24	63			+0.5 -0.5

Continued on next page. . .

Table 2 – Continued

#	Location		Preferred start date	reference	Preferred end date	reference	Preferred duration (days)	Duration U/C (days) Start	End	Max
62	E flank	(B)	13/05/2008	[25,26,27]	06/07/2009	[25,26,27]	419		-2	*+0.5* -2

Reference numbers correspond to the following sources: [1]Tanguy et al. (2007), [2]Tanguy (1981), [3]Branca and Del Carlo (2004), [4]Mulargia et al. (1985), [5]Behncke et al. (2005), [6]Branca and Del Carlo (2005), [7]Chester et al. (2012), [8]Behncke and Neri (2003), [9]Andronico and Lodato (2005), [10]Acocella and Neri (2003), [11]Neri et al. (2011); [12]Chester et al. (1999), [13]Wadge (1976), [14]Tanguy et al. (1973), [15]Wadge and Guest (1981), [16]Le Guern (1972), [17]Guerra et al. (1976), [18]Pinkerton and Sparks (1976), [19]Harris et al. (2000), [20]Coltelli et al. (2007), [21]Corsaro and Miraglia (2009), [22]Burton et al. (2005), [23]Neri and Acocella (2006), [24]Behncke et al. (2009), [25]Bonaccorso et al. (2011a), [26]Branca et al. (2008), [27]Bonaccorso et al. (2011b). Bracketed letters represent the sector that the eruptive fissure/vent belongs, according to Fig 1. U/C represents uncertainty and italicized values are those assigned according to the method in Table 1

553

Table 3: Mantel-Haenszel Logrank test results for all possible sector pairs

#	Sector Pair	χ^2	P Value
1	A-B	0.5	0.465
2	B-C	0.0	0.988
3	A-C	0.0	0.870

* = X^2 significant at the 5 % level

Table 4: Table showing the forecast results for the 1600-2010 and 1670-2010 datasets using (a) survivor function models, (b) residual life function models where t = 14 days and (c) quantile function models. The first column refers to the scenario being forecast where x is the total eruption duration and p the quantile of interest. CI represents the confidence interval

(a) 1600-2010 Survivor Function

x	**Result**	**95% CI**	**80% CI**
7 days	84%	± 8%	± 5%
30 days	57%	± 11%	± 7%
365 days	11%	± 6%	± 4%

(b) 1670-2010 Survivor Function

x	**Result**	**95% CI**	**80% CI**
7 days	82%	± 9%	± 6%
30 days	52%	± 12%	± 8%
365 days	8%	± 5%	± 4%

(c) 1600-2010 Residual life Function

x	**Result**	**95% CI**	**80% CI**
21 days	89%	± 6%	± 4%
74 days	50%	± 10%	± 7%

(d) 1670-2010 Residual life Function

x	**Result**	**95% CI**	**80% CI**
21 days	87%	± 6%	± 4%
74 days	44%	± 10%	± 7%

(e) 1600-2010 Quantile Function

p	**Result (days)**	**95% CI (days)**	**80% CI (days)**
0.34	20	± 10	± 7
0.67	86	± 44	± 29

(f) 1670-2010 Quantile Function

p	**Result (days)**	**95% CI (days)**	**80% CI (days)**
0.34	17	± 9	± 6
0.67	67	± 34	± 22

Table 5: Table containing the equations involved in calculating variance ($\hat{V}$) for the Log-logistic distribution in the survivor function ($\hat{F}(x)$), residual life function ($\hat{F}_t$) and quantile function (x_p) models

	Equation
($\hat{V}$)	$D^2\,C[1,1] + E\,C^2[2,2] + 2DE\,C[1,2]$
($\hat{F}(x)$)	$D = -\frac{(x/\sigma)^\beta\, log(x/\sigma)}{\{1+(x/\sigma)^\beta\}^2}$ $E = \frac{\beta}{\sigma}\,\frac{(x/\sigma)^\beta}{\{1+(x/\sigma)^\beta\}^2}$
($\hat{F}_t$)	$D = \frac{(xt)^\beta\, log(t/x)+(\sigma t)^\beta\, log(t/\sigma)-(\sigma x)^\beta\, log(x/\sigma)}{(\sigma^\beta+x^\beta)^2}$ $E = \frac{\beta\sigma^{\beta-1}(x^\beta-t^\beta)}{(\sigma^\beta+x^\beta)^2}$
(x_p)	$D = -\frac{\sigma}{\beta^2}\left(\frac{p}{1-p}\right)^{1/\beta} log\left(\frac{p}{1-p}\right)$ $E = \left(\frac{p}{1-p}\right)^{1/\beta}$

References

Acocella, V. and Neri, M. (2003). What makes flank eruptions? The 2001 Etna eruption and its possible triggering mechanisms. *Bull Volcanol*, 65(7):517–529.

Allard, P., Behncke, B., D'Amico, S., Neri, M., and Gambino, S. (2006). Mount Etna 1993-2005: Anatomy of an evolving eruptive cycle. *Earth-Science Reviews*, 78(1-2):85–114.

Andronico, D. and Lodato, L. (2005). Effusive activity at Mount Etna volcano (Italy) during the 20th Century: A contribution to volcanic hazard assesment. *Nat Hazards*, 36:407–443.

Bebbington, M. S. and Lai, C. D. (1996). Statistical analysis of New Zealand volcanic occurrence data. *J Volcanol Geoth Res*, 74(1-2):101–110.

Behncke, B., Falsaperla, S., and Pecora, E. (2009). Complex magma dynamics at Mount Etna revealed by seismic, thermal, and volcanological data. *J Geophys Res*, 114:1–17.

Behncke, B. and Neri, M. (2003). Cycles and trends in the recent eruptive behaviour of Mount Etna (Italy). *Can J Earth Sci*, 40(10):1405–1411.

Behncke, B., Neri, M., and Nagay, A. (2005). Lava flow hazard at Mount Etna (Italy): New data from a GIS-based study. In Manga, M. and Ventura, G., editors, *Kinematics and Dynamics of Lava Flows*, pages 189–208. GSAMSP369, Boulder, Colorado.

Benoit, J. P. and McNutt, S. R. (1996). Global volcanic earthquake swarm database and preliminary analysis of volcanic earthquake swarm duration. *Ann Geofis*, XXXIX:221–229.

Bisson, M., Behncke, B., Fornaciai, A., and Neri, M. (2009). LiDAR-based digital terrain analysis of an area exposed to the risk of lava flow invasion: the Zafferana Etnea territory, Mt. Etna (Italy). *Nat Hazards*, 50(2):321–334.

575 Bonaccorso, A., Bonforte, A., Calvari, S., Del Negro, C., Di Grazia, G., Ganci, G., Neri, M.,
576 Vicari, A., and Boschi, E. (2011a). The initial phases of the 2008 - 2009 Mount Etna eruption:
577 A multidisciplinary approach for hazard assessment. *J Geophys Res*, 116:1–19.

578 Bonaccorso, A., Cannata, A., Corsaro, R. A., Di Grazia, G., Gambino, S., Greco, F., Miraglia, L.,
579 and Pistorio, A. (2011b). Multidisciplinary investigation on a lava fountain preceding a flank
580 eruption: The 10 May 2008 Etna case. *Geochem, Geophys, Geosyst*, 12(7):1–21.

581 Branca, S., Coltelli, M., De Beni, E., and Wijbrans, J. (2008). Geological evolution of Mount Etna
582 volcano (Italy) from earliest products until the first central volcanism (between 500 and 100 ka
583 ago) inferred from geochronological and stratigraphic data. *Int J Earth Sci*, 97(1):135–152.

584 Branca, S., Coltelli, M., Groppelli, G., and Lentini, F. (2011). Geological map of Etna volcano, 1 :
585 50, 000 scale. *Ital J Geosci*, 130(3):265–291.

586 Branca, S. and Del Carlo, P. (2004). Eruptions of Mt. Etna during the past 3200 years: A revised
587 compilation integrating the historical and stratigraphical records. In Bonaccorso, A., Calvari,
588 S., Coltelli, M., Negro, C. D., and Falsaperla, S., editors, *Mt. Etna: Volcano Laboratory*, pages
589 1–22. Am Geophys Union, Washington, United States.

590 Branca, S. and Del Carlo, P. (2005). Types of eruptions of Etna volcano AD 1670-2003: implica-
591 tions for short-term eruptive behaviour. *Bull Volcanol*, 67(8):732–742.

592 Budescu, D. V., Broomell, S., and Por, H. H. (2009). Improving communication of uncertainty in
593 the reports of the Intergovernmental Panel on Climate Change. *Psychol Sci*, 20(3):299–308.

594 Burton, M. R., Neri, M., Andronico, D., Branca, S., Caltabiano, T., Calvari, S., Corsaro, R. A., Del
595 Carlo, P., Lanzafame, G., Lodato, L., Miraglia, L., Salerno, G., and Spampinato, L. (2005). Etna
596 2004-2005: An archetype for geodynamically-controlled effusive eruptions. *Geophys Res Lett*,
597 32(9):1–4.

598 Cappello, A., Bilotta, G., Neri, M., and Negro, C. D. (2013). Probabilistic modeling of future
599 volcanic eruptions at Mount Etna. *JGR-se*, 118(5):1925–1935.

600 Cappello, A., Neri, M., Acocella, V., Gallo, G., Vicari, A., and Del Negro, C. (2012). Spatial vent
601 opening probability map of Etna volcano (Sicily, Italy). *Bull Volcanol*, 74(9):2083–2094.

602 Chester, D. K., Duncan, A. M., Dibben, C., Guest, J. E., and Lister, P. H. (1999). Mascali, Mount
603 Etna region Sicily: An example of fascist planning during the 1928 eruption and its continuing
604 legacy. *Nat Hazards*, 19(1):29–46.

605 Chester, D. K., Duncan, A. M., Guest, J. E., and Kilburn, C. R. J. (1985). *Mount Etna The anatomy*
606 *of a volcano*. Chapman and Hall, London.

607 Chester, D. K., Duncan, A. M., and Sangster, H. (2012). Human responses to eruptions of Etna
608 (Sicily) during the late-pre-industrial era and their implications for present-day disaster planning.
609 *J Volcanol Geoth Res*, 225-226:65–80.

610 Coltelli, M., Proietti, C., Branca, S., Marsella, M., Andronico, D., and Lodato, L. (2007). Analysis
611 of the 2001 lava flow eruption of Mt. Etna from three-dimensional mapping. *J Geophys Res*,
612 112:1–18.

613 Corsaro, R. and Miraglia, L. (2009). Dynamics of magma in the plumbing system of Mt. Etna
614 volcano, Sicily, Italy: A contribution from petrologic data of volcanics erupted from 2007 to
615 2009. In *American Geophysical Union, Fall Meeting, abstract # V51C-1690*.

616 Crisci, G. M., Avolio, M. V., Behncke, B., D'Ambrosio, D., Di Gregorio, S., Lupiano, V., Neri, M.,
617 Rongo, R., and Spataro, W. (2010). Predicting the impact of lava flows at Mount Etna, Italy. *J*
618 *Geophys Res*, 115(B4):B04203.

619 Duncan, A. M., Chester, D. K., and Guest, J. E. (1981). Mount Etna volcano: Environmental

620 impact and problems of volcanic prediction. *The Geogr J*, 147(2):164–178.

621 Frazzetta, G. and Romano, R. (1978). Approccio di studio per la stesura di una carta del rischio
622 vulcanico (Etna-Sicilia). *Memorie della Società Geologica Italiana*, 19:691–697.

623 Guerra, I., Lo Bascio, A., Luongo, G., and Scarpa, R. (1976). Seismic activity accompanying the
624 1974 eruption of Mt. Etna. *J Volcanol Geoth Res*, 1(4):347–362.

625 Guest, J. E., Chester, D. K., and Duncan, A. M. (1984). The Valle del Bove Mount Etna: Its origin
626 and relation to the stratigraphy and structure of the volcano. *J Volcanol Geoth Res*, 21:1–23.

627 Guest, J. E. and Murray, J. B. (1979). An analysis of hazard from Mount Etna volcano. *J Geol Soc*
628 *London*, 136:347–354.

629 Harris, A. J. L., Favalli, M., Wright, R., and Garbeil, H. (2011). Hazard assessment at Mount Etna
630 using a hybrid lava flow inundation model and satellite-based land classification. *Nat Hazards*,
631 58(3):1001–1027.

632 Harris, A. J. L., Murray, J. B., Aries, S. E., Davies, M. A., Flynn, L. P., Wooster, M. J., Wright,
633 R., and Rothery, D. A. (2000). Effusion rate trends at Etna and Krafla and their implications for
634 eruptive mechanisms. *J Volcanol Geoth Res*, 102:237–269.

635 Hughes, J. W., Guest, J. E., and Duncan, A. M. (1990). Changing styles of effusive eruption on
636 Mount Etna since AD 1600. *Magma Transport and Storage. Wiley, New York*, pages 385–406.

637 Le Guern, F. (1972). Etudes dynamiques sur la phase gazeuse éruptive. Technical report, Commis-
638 sariat à l'Energie Atomique, France.

639 Machin, D., Cheung, Y., and Parmar, M. K. B. (2006). *Survival analysis: A practical approach*.
640 Wiley, second edition.

641 Marzocchi, W. and Bebbington, M. (2012). Probabilistic eruption forecasting at short and long
642 time scales. *Bull Volcanol*, 74(8):1777–1805.

643 Mastrandrea, M. D., Field, C. B., Stocker, T. F., Edenhofer, O., Ebi, K., Frame, D., Held, H.,
644 Kriegler, E., Mach, K., Matschoss, P., Plattner, G., Yohe, G., and Zwiers, F. (2010). Guidance
645 note for lead authers of the IPCC fifth assessment report on consistent treatment of uncertainties.
646 Technical report, Intergovernmental Panel on Climate Change (IPCC).

647 Mulargia, F., Tinti, S., and Boschi, E. (1985). A statistical analysis of flank eruptions on Etna
648 volcano. *J Volcanol Geoth Res*, 23(3-4):263–272.

649 Neri, M. and Acocella, V. (2006). The 2004-2005 Etna eruption: Implications for flank deformation
650 and structural behaviour of the volcano. *J Volcanol Geoth Res*, 158(1):195–206.

651 Neri, M., Acocella, V., Behncke, B., Giammanco, S., Mazzarini, F., and Rust, D. (2011). Structural
652 analysis of the eruptive fissures at Mount Etna (Italy). *Ann Geophys*, 65(5):464–479.

653 Passarelli, L., Sansò, B., Sandri, L., and Marzocchi, W. (2010). Testing forecasts of a new Bayesian
654 time-predictable model of eruption occurrence. *J Volcanol Geoth Res*, 198(1-2):57–75.

655 Patané, D., Gori, P. D., Chiarabba, C., and Bonaccorso, A. (2003). Magma ascent and the pressur-
656 ization of Mount Etna's volcanic system. *Science*, 299(5615):2061–2063.

657 Pinkerton, H. and Sparks, R. S. J. (1976). The 1975 sub-terminal lavas, Mount Etna: a case history
658 of the formation of a compound lava field. *J Volcanol Geoth Res*, 1(2):167–182.

659 Proietti, C., De Beni, E., Coltelli, M., and Branca, S. (2011). The flank eruption history of Etna
660 (1610-2006) as a constraint on lava flow hazard. *Ann Geophys*, 54(5):480–490.

661 Romano, R., Sturiale, C., and Lentini, F. (1979). *Geological Map of Mt. Etna*. CNR, Progetto
662 Finalizzato Geodynamica, Instituto Internazionale di Vulcanologia (Catania). 1:50.000 scale.

663 Salvi, F., Scandone, R., and Palma, C. (2006). Statistical analysis of the historical activity of Mount
664 Etna, aimed at the evaluation of volcanic hazard. *J Volcanol Geoth Res*, 154:159–168.

665 Siebert, L., Simkin, T., and Kimberley, P. (2010). *Volcanoes of the World*. Smithsonian Institution,
666 Washington, D.C., 3rd edition.

667 Simkin, T. (1993). Terrestrial volcanism in space and time. *Earth Planet Sc Lett*, 21:427–452.

668 Smethurst, L., James, M. R., Pinkerton, H., and Tawn, J. A. (2009). A statistical analysis of eruptive
669 activity on Mount Etna, Sicily. *Geophys J Int*, 179(1):655–666.

670 Sparks, R. S. J. and Aspinall, W. P. (2004). Volcanic Activity : Frontiers and Challenges in Fore-
671 casting , Prediction and Risk Assessment. In Sparks, R. S. J. and Hawkesworth, C. J., editors,
672 *The state of the planet: Frontiers and Challenges in Geophysics*, pages 359–373. IUGG/AGU.

673 Stieltjes, L. and Moutou, P. (1989). A statistical and probabilistic study of the historic activity of
674 Piton de la Fournaise, Reunion Island, Indian Ocean. *J Volcanol Geoth Res*, 36(1-3):67–86.

675 Tanguy, J. (1981). Les éruptions historiques de l'Etna: chronologie et localisation. *Bulletin Vol-
676 canologique*, 44(3):585–640.

677 Tanguy, J.-C., Condomines, M., Le Goff, M., Chillemi, V., La Delfa, S., and Patanè, G. (2007).
678 Mount Etna eruptions of the last 2,750 years: revised chronology and location through archeo-
679 magnetic and ^{226}Ra-^{230}Th dating. *Bull Volcanol*, 70(1):55–83.

680 Tanguy, J.-C., Le Goff, M., Principe, C., Arrighi, S., Chillemi, V., Paiotti, A., La Delfa, S., and
681 Patanè, G. (2003). Archeomagnetic dating of Mediterranean volcanics of the last 2100 years:
682 Validity and limits. *Earth Planet Sc Lett*, 211(1-2):111–124.

683 Tanguy, J. C., Tazieff, H., and Cristofolini, R. (1973). The 1971 Etna Eruption: Petrography of the
684 Lavas [and discussion]. *Philos T Roy Soc A*, 274(1238):45–53.

685 Venzke, E., Wuderman, R. W., McClelland, L., Simkin, T., Luhr, J. F., Siebert, L., Mayberry,
686 G., and Sennert, S. (2002). Global Volcanism Program Digital Information Series. `http:`
687 `//www.volcano.si.edu/reports/`. Last Accessed: 01-08-2012.

688 Wadge, G. (1976). Deformation of Mount Etna, 1971-1974. *J Volcanol Geoth Res*, 1(3):237–263.

689 Wadge, G. and Guest, J. E. (1981). Steady-state magma discharge at Etna 1971-81. *Nature*,
690 294(5841):548–550.

691 Wadge, G., Walker, G. P. L., and Guest, J. E. (1975). The output of the Etna volcano. *Nature*,
692 255(5507):385–387.